Available online at www.sciencedirect.com
SCIENCE DIRECT®
Dyes and Pigments 66 (2005) 61–68
DYES and PIGMENTS
www.elsevier.com/locate/dyepig

The photosensitization activity of a water-soluble carboxylate of hypocrellin B

Yuewei Zhao, Jie Xie, Jingquan Zhao*

Key laboratory of Photochemistry, Center for Molecular science, Institute of Chemistry, The Chinese Academy of Sciences, Beijing 100080, PR China

Received 27 March 2004; received in revised form 15 May 2004; accepted 11 August 2004
Available online 20 October 2004

Abstract

Based on theoretical prediction of the molecular polarity, water-soluble sodium HB-14-carboxylate (SCHB) was prepared and its photosensitization activity was evaluated. SCHB shows not only very good amphiphilicity but also much stronger absorption at 620 nm than its parents. In DMSO–PBS (3:1 by volume) solution (pH 7.4) of SCHB, the photosensitization generated the semiquinone anion radicals ($SCHB^{\bullet -}$) under anaerobic condition or superoxide anion radicals ($O_2^{\bullet -}$) in the presence of oxygen. In the oxygenated PBS solution of SCHB, hydroxyl radicals ($^{\bullet}OH$) were photogenerated. In addition, SCHB could also be photosensitized to generate singlet oxygen ($^1O_2$) with a quantum yield about 0.26. These findings suggest that SCHB can exert photodynamic action via photosensitization.
© 2004 Elsevier Ltd. All rights reserved.

Keywords: Hypocrellin; Photosensitization activity; Molecular polarity; Phototherapeutic window; Electronic paramagnetic resonance; Amphiphilicity

1. Introduction

In recent years, it has been realized that it is a new strategy to develop specially used photodynamic medicines according to the particularities of the diseases. Such as, for photodynamic therapy of solid tumors, the medicine should possess a strong light absorption on the phototherapeutic window (600 nm–900 nm), on the other hand, for photodynamic therapy of superficial or early stage tumors as well as vascular–capillary diseases, occurred no deeper than 1 mm, the phototherapeutic window should be on the range of around 500 nm because a deeper penetrate light may be harmful to the normal tissue. Hypocrellins, well known for their photodynamic activities to tumors and viruses [1–3], possess the main absorption mainly over 450 nm–550 nm, which is shortcoming for phototherapy of solid tumors but it coincides with the phototherapeutic window of vascular–capillary diseases, such as, port wine stain and age-related macular degeneration (AMD), as well as the superficial or early stage tumors. On the other hand, hypocrellins show very good cellular uptake but tend to self-aggregate in blood as well as in aqueous solution, while the completely water-soluble derivatives show very poor cellular uptake so very low photodynamic activity [4]. Therefore, to make a compromise between cellular uptake (lipophilicity) and the fluent transportation in vascular net (hydrophilicity) is an important factor for hypocrellins to be clinically applicable [5]. In previous work, we developed a theoretical method for prediction of the polarity of a hypocrellin derivative, defined as an averaged net charge/atom for each molecule. The amphiphilicity of a molecule was evaluated by the polarity based on the comparison of the calculated

* Corresponding author. Fax: +86 10 82617315.
E-mail address: zhaojq@iccas.ac.cn (J. Zhao).

0143-7208/$ - see front matter © 2004 Elsevier Ltd. All rights reserved.
doi:10.1016/j.dyepig.2004.08.015

values with the available experimental partition coefficient between organic solvent and aqueous solution. For about 50 compounds, the polarity values fall on a range from 0.18 (liposoluble only) to 0.24 (water-soluble only). The calculated values agree very well with the experimental partition coefficients. It was predicated that a derivative with the polarity value about 0.22 would possess best amphiphilicity [6]. In the current work, the polarity value of sodium carboxylate at position 14 of HB (SCHB) was estimated to be 0.219. Therefore, this derivative was chosen as a candidate to be prepared. As expected, the experimentally measured partition coefficient did agree well with the polarity value. Furthermore, the chemical reactive species, semiquinone anion radicals, superoxide anion radicals, hydroxyl radicals and singlet oxygen, generated through photosensitization of SCHB were detected by electronic paramagnetic resonance (EPR) and spectrophotometric measurements.

2. Experimental

2.1. Materials and general methods

HB was prepared as described previously [7]. 5,5-Dimethyl-1-pyrroline-*N*-oxide (DMPO), 9,10-diphenylanthracene (DPA), 2,2,6,6-tetramethyl-4-piperidone (TEMP) and 2,2,6,6-tetramethyl-4-piperidone-*N*-oxyl radical (TEMPO) were purchased from Aldrich Chemical Company. Catalase, Rose Bengal (RB), cytochrome *c* (horse heart) and superoxide dismutase (SOD) were purchased from Sigma Chemical Company. Cysteine, reduced glutathione (GSH), reduced nicotinamide adenine dinucleotide (NADH) were obtained from Biochem. Technology Corporation, the Chinese Academy of Sciences. 1,4-Diazabicyclo [2,2,2] octane (DABCO) and diethylene triamine pentaacetic acid (DTPA) were purchased from Merck Chemical Company. Other agents of analytical grades were purchased from Beijing Chemical Plant. HBO_2H was synthesized according to Ref. [8] and characterized by the use of IR, H NMR and MS (FAB) spectroscopy. Phosphate buffer saline (PBS) solutions under different pH value were prepared by adjusting with 10 mM KH_2PO_4 and 10 mM Na_2HPO_4 solution. The working solutions were prepared immediately and water was freshly distilled before use. The solutions were purged with oxygen, air or argon according to the experimental requirements.

2.2. Spectroscopic and EPR measurements

The absorption spectra were recorded on a Shimadzu UV-1601 spectrophotometer. A 450 W medium pressure sodium lamp was used as light source and a long pass filter was employed to eliminate light of wavelength shorter than 470 nm. Fluorescence emission and excitation spectra were obtained on a Hitachi F-4500 spectrofluorimeter.

The EPR measurements were performed on a Bruker ESP-300E spectrometer at room temperature. Unless indicated, the instrumental settings were: microwave power, 10.02 mW (3.17 mW for the $^{\bullet}OH$ signal); modulation amplitude, 1.012 G; sweep width, 100 G (50 G for semiquinone radical signal) and receiver gain, 1.0×10^5 (1.0×10^4 for $^{\bullet}OH$). A 532 nm YAG-900 laser (Spectro-Physics Laser, Mountain View, CA, USA) was used as the light source. Samples were injected into quartz capillaries designed specially for EPR analysis. Anaerobic or aerobic samples were prepared by purging the reactive volume with argon or oxygen and stored in the dark for 30 min. EPR signals were recorded and manipulated in an IBM/PC computer. Kinetics of spin adduct generation was studied based on the recorded peak value of an EPR spectrum every 10 s.

3. Results and discussion

3.1. The preparation of SCHB and the partition coefficients (PC)

SCHB was prepared through the reaction of HBO_2H (558 mg, 1 mMol) with NaOH (40 mg, 1 mMol) in redistilled water (1 mL) with stirring vigorously for 1 h at room temperature in the dark. The stored solution of 1 M SCHB was used for further dilution to any lower concentrations with PBS or DMSO–PBS mixed solution. Fig. 1B shows the absorption spectrum of SCHB and also those of HBO_2H under alkaline condition (pH higher than 9.0) and in saturated NaCl solution. Based on these, it is confirmed that SCHB obtained from the above procedure is a new product instead of that formed in different pH or ionic strength condition.

The values of partition coefficients (PC) were determined by distribution of photosensitizers between the *n*-octanol and PBS solution (pH 7.4) [5]. The PC values for HBO_2H, SCHB (Scheme 1), HA and HB were listed in the Table 1. It can be seen that the hydrophilicity of SCHB is enhanced greatly compared to HB and HBO_2H. It should be indicated that SCHB still possesses superior distribution in organic phase, which is beneficial to the cellular uptake. On the other hand, SCHB can be easily dissolved in the aqueous phosphate buffer solution, which is beneficial to transportation in vascular net.

The absorption spectra of SCHB and HBO_2H are shown in Fig. 1A. Compared with that for HBO_2H, the absorption spectrum of SCHB does not change much, however, a moderate-strength peak appears at 620 nm, which is attractive for the therapy of solid tumors. The fluorescent spectrum is mainly unchanged.

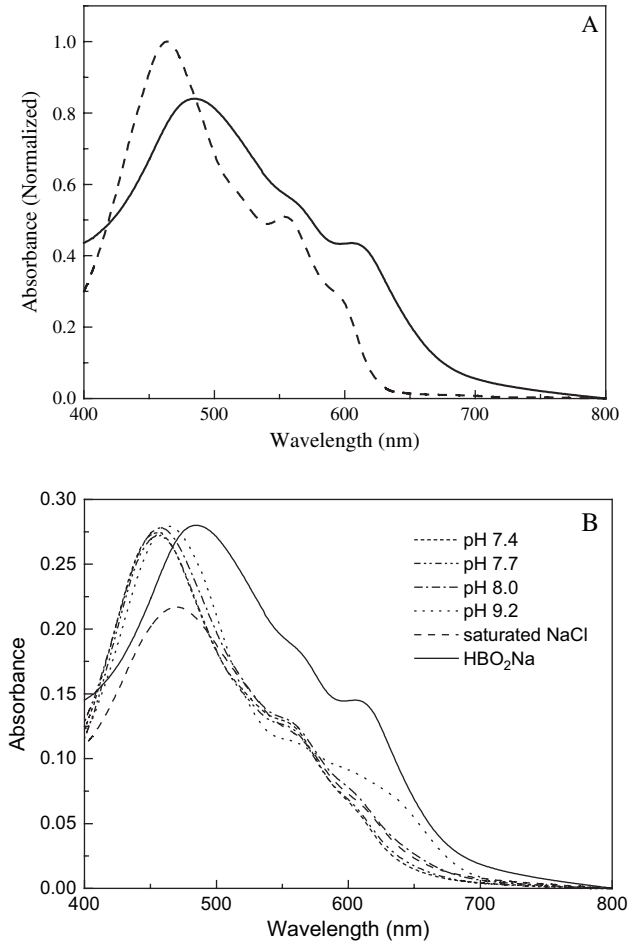

Fig. 1. (A) Absorption spectra of HBO_2H (–) and SCHB (—) in PBS solution (pH 7.4) at the same concentration (1 mM). (B) Absorption spectra of SCHB and HBO_2H under different pH value solution or saturated NaCl solution.

3.2. Photo-induced generation of semiquinone anion radicals by SCHB

As shown in Fig. 2A, irradiating the deoxygenated DMSO–PBS (3:1 by volume) solution (pH 7.4) of SCHB (1 mM) produced a strong EPR signal ($g = 2.0058$). The control experiments proved that illumination and SCHB were essential. With the addition of NADH (50 μM), a typical electron donor, an EPR signal (Fig. 2B) similar to that in Fig. 2A was produced but the intensity was enhanced significantly. Control experiments showed that the signal did not appear without SCHB or/and illumination. A series of electron donors (D) with different redox potentials were tested in place of NADH. The EPR signal was similar to that in Fig. 2A but the intensities increased sharply with the decrease in redox potentials of the donors (Table 2), confirming the anionic nature of the radicals.

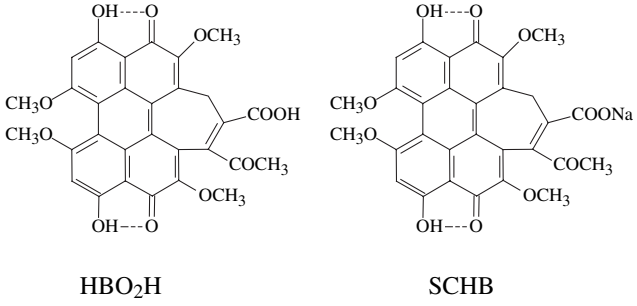

Scheme 1.

Table 1
Partition coefficients (PC) of hypocrellin dyes

Compound	HA	HB	HBO_2H	SCHB
PC	41.6 [12]	46.4 [12]	11.598	4.25

The signal in Fig. 2(B) could be readily ascribed to the semiquinone anion radicals of SCHB ($SCHB^{\bullet -}$) formed by the electron transfer from an electron donor to the triplet SCHB [9–11].

The EPR signal intensity in Fig. 2A depends on irradiation time, intensity (inset a) and SCHB concentration (inset b). Considering the similarity, the radicals may be ascribed to the semiquinone anion radicals of SCHB ($SCHB^{\bullet -}$) generated via the self-electron transfer between the excited triplet state and the ground state species [4].

The EPR signal in Fig. 2A would disappear in the oxygenated solution, as shown in Fig. 2C, while the DMPO-$O_2^{\bullet -}$ adducts were generated with the existence of DMPO, further confirming the signal originated from the semiquinone anion radicals of SCHB ($SCHB^{\bullet -}$). Because of the anionic nature, the radicals are stable in anaerobic and aprotic solvent, such as DMSO. In the DMSO–PBS (3:1 by volume) solution (pH 7.4), the

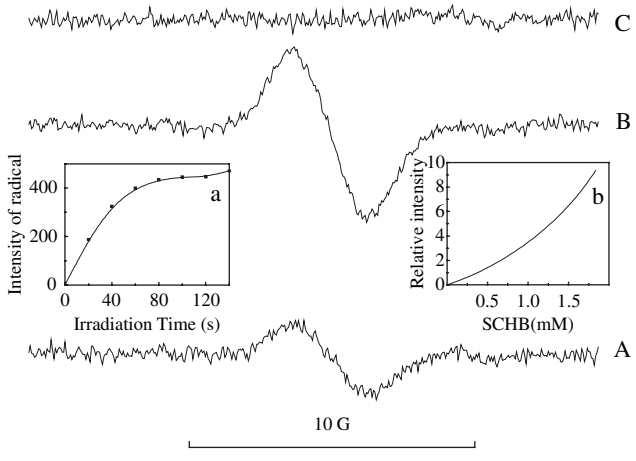

Fig. 2. (A) EPR spectrum for deoxygenated DMSO–PBS (3:1 by volume) solution (pH 7.4) of SCHB (1 mM) under irradiation for 1 min with laser of 532 nm. (B) The same as (A) but with the presence of NADH (50 μM). (C) The same as (A) but oxygen was bubbled through the solution after illumination.

Table 2
Effect of electron donors with different redox potentials on the intensity of the EPR signal intensity of the semiquinone anion radicals

Electron donor	Signal intensity	$E_{(D^{\bullet+}/D)}$ (V)
SCHB	162	–
Glutathione	245	0.87
Cysteine	318	0.63
NADH	467	0.28

EPR signal of $SCHB^{\bullet-}$ was still observable, however, when the solution was replaced with the entirely aqueous PBS solution, the signal for semiquinone anion radicals was not detectable by EPR or spectrophotometer [7,12].

It was reported that the anionic radicals of a photosensitizer generated in the PBS solution could be detected by using the spin counteraction of TEMPO [9]. When the deoxygenated PBS solution (pH 7.4) of SCHB (1 mM) and TEMPO (50 μM) was irradiated, the EPR signal intensity of TEMPO decreased exponentially with illumination time (Fig. 3), confirming the photogeneration of $SCHB^{\bullet-}$ in PBS solution. The failure to detect $SCHB^{\bullet-}$ by steady state EPR was most likely due to the shorter lifetime in the PBS solution [13].

The decay kinetics of the semiquinone anion radicals ($SCHB^{\bullet-}$) was studied by recording the decrease in EPR signal intensity after illumination, shown in Fig. 4. The decay curve (line 1) for $SCHB^{\bullet-}$ in the deoxygenated DMSO–PBS (3:1 by volume) solution (pH 7.4) obeys second-order kinetics in the absence of an electron donor, described by Eq. (1), while the line 2 for that in the presence of NADH also obeys second-order kinetics but with much faster decay rate. In fact, in the presence of electron donor, $SCHB^{\bullet-}$ should decay via the second- and first-order kinetics described by Eqs. (1) and (2), respectively. The observed second-order kinetic decay of

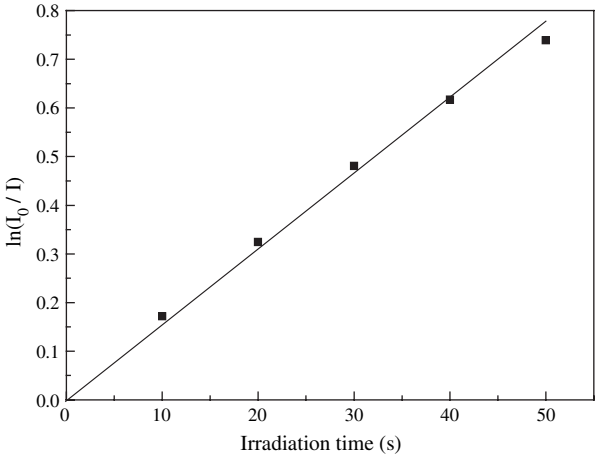

Fig. 3. The decay of TEMPO (50 μM) signal intensity (I) via spin counteraction to $SCHB^{\bullet-}$ photogenerated by SCHB (1 mM) in the deoxygenated PBS solution (pH = 7.4).

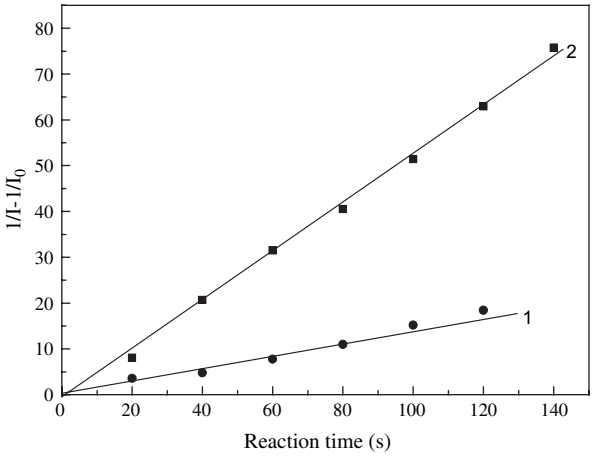

Fig. 4. Line 1: Dependence of the reciprocal of the EPR signal intensity (I) for $SCHB^{\bullet-}$ on the time after irradiation in the deoxygenated DMSO–PBS (3:1 by volume) solution (pH 7.4) of SCHB (1 mM). Line 2: The same as line 1 but in the presence of NADH (50 μM).

$SCHB^{\bullet-}$ suggested that Eq. (1) should be the dominant pathway under our experimental conditions.

$$SCHB^{\bullet-} + SCHB^{\bullet-} \xrightarrow{H^+} SCHBH_2 + SCHB \quad (1)$$

$$SCHB^{\bullet-} + D \xrightarrow{H^+} SCHBH_2 + D^+ \quad (2)$$

3.3. Generation of superoxide anion radical ($O_2^{\bullet-}$) by SCHB

As mentioned previously, the EPR signal for $SCHB^{\bullet-}$ would disappear in the oxygenated solution, while an EPR signal with a feature of coupling with one nitrogen and two hydrogen atoms at the β and γ positions appeared immediately in the presence of DMPO (50 mM) (Fig. 5A and Fig. 6 line 1). The g factor and parameters ($g = 2.0048$, $\alpha^N = 12.89$ G, $\alpha_\beta^H = 10.62$ G, $\alpha_\gamma^H = 1.45$ G) were in good agreements with those reported for DMPO-$O_2^{\bullet-}$ radical adducts [14]. Control experiments showed that SCHB, oxygen and illumination were all necessary for the EPR signal (Fig. 5D). Addition of SOD (20 μg/mL) inhibited the EPR signal effectively (Fig. 5C and Fig. 6 line 2), whereas thermally denatured SOD had no effect, further confirming the formation of $O_2^{\bullet-}$.

Addition of DABCO (10 mM) or histidine (10 mM), commonly used to inhibit $^1O_2$-dependent reactions [15], did not affect the EPR signal intensity, suggesting that $^1O_2$ was not involved in the formation of $O_2^{\bullet-}$. The EPR signal was greatly intensified (Fig. 5B and Fig. 6 line 3) in the presence of NADH (50 μM). Control experiments showed that light, oxygen and SCHB were all necessary even in the presence of electron donors. The consistent

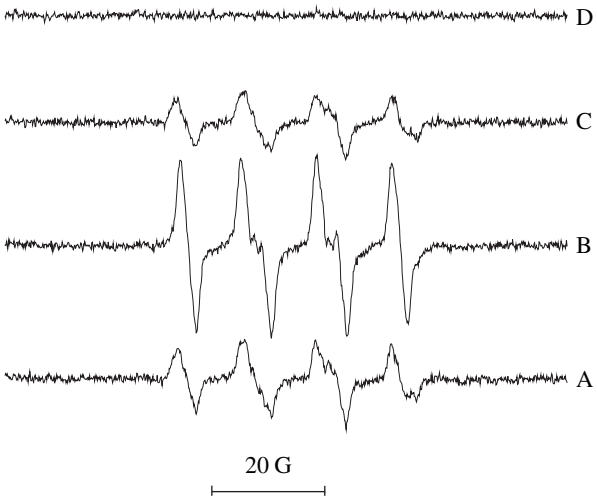

Fig. 5. (A) EPR spectrum of DMPO-suprexoide radical adducts produced by irradiation of the oxygen-saturated DMSO–PBS (3:1 by volume) solution (pH 7.4) of SCHB (1 mM) and DMPO (50 mM) for 1 min. (B) The same as (A) but in the presence of NADH (50 μM). (C) The same as (A) but in the presence of SOD (20 μg/mL). (D) The same as (A) but in the absence of SCHB, oxygen or irradiation.

enhancement effects of electron donors on the formations of $O_2^{\bullet-}$ and $SCHB^{\bullet-}$ suggested that $O_2^{\bullet-}$ must originate from $SCHB^{\bullet-}$. Besides, it may be also possible that $O_2^{\bullet-}$ is generated via the electron transfer from electron donors or triplet photosensitizer to O_2 [10,16]. Fig. 6 shows the dependence of the EPR signal intensity on the irradiation time.

The reduction of Cyt Fe^{3+} by $O_2^{\bullet-}$ is usually used to monitor the formation and accumulation of $O_2^{\bullet-}$ [11,17–21]. Fig. 7 shows the absorption spectra of reduced cytochrome *c* in an oxygen-saturated DMSO–PBS (3:1 by volume) solution (pH 7.4) of

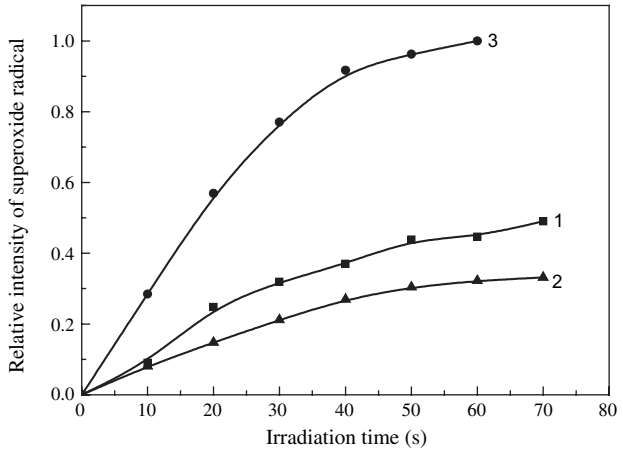

Fig. 6. Line 1: Dependence of the EPR signal intensity of the DMPO-superoxide spin-adducts on the irradiation time in the oxygen-saturated DMSO–PBS (3:1 by volume) solution (pH 7.4) of SCHB (1 mM) and DMPO (50 mM). Line 2: The same as line 1 but in the presence of SOD (20 μg/mL). Line 3: The same as line 1 but in the presence of NADH (50 μM).

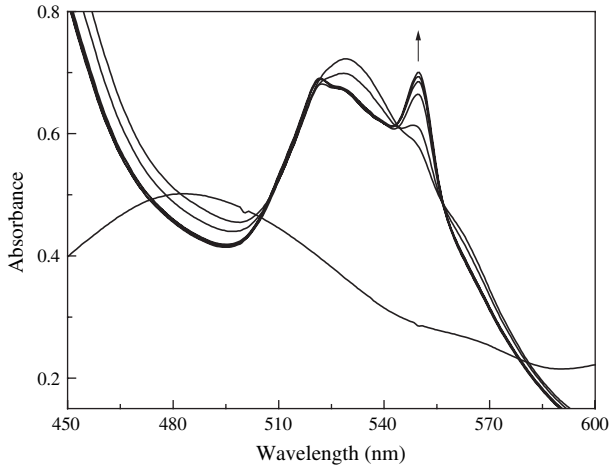

Fig. 7. Absorbance spectra of the oxygen-saturated DMSO–buffer (3:1 by volume) solution (pH 7.4) containing SCHB (1 mM) and cytochrome *c* (80 μM) under irradiation for 0, 10, 20, 30, 40, 50 and 60 s. The arrow indicates the direction of change.

SCHB (1 mM) and cytochrome *c* (80 μM) under irradiation. The increase in absorbance at 550 nm is the characteristic of the reduction of Cyt Fe^{3+}, corresponding to the formation and accumulation of $O_2^{\bullet-}$. Control experiments confirmed that SCHB and light were essential for the reduction of cytochrome *c*.

3.4. Photogeneration of hydroxyl radicals $^{\bullet}OH$

When SCHB (1 mM) and DMPO (50 mM) were dissolved in the PBS solution instead of PBS-DSMO mixed solution, a four-line EPR spectrum (Fig 8A) with hyperfine splitting constants of $\alpha^N = \alpha^H = 14.87$ G, characteristic of the DMPO-$^{\bullet}$OH spin adducts [22–25], was recorded under 1 min irradiation, while the signal for DMPO-$O_2^{\bullet-}$ disappeared. The signal intensity increased with the concentration of SCHB (Fig. 8B) and the irradiation time (Fig. 9 line 1). Control experiments demonstrated that light, oxygen, SCHB and DMPO were all necessary. Histidine and DABCO, $^1O_2$ quenchers, did not have any effect on the EPR signal intensity of the DMPO-$^{\bullet}$OH adducts, indicating that $^1O_2$ was not involved in the formation of $^{\bullet}$OH [25]. When ethanol (0.1 M) was introduced into the solution prior to illumination, the signal of DMPO-$^{\bullet}$OH disappeared while the EPR spectrum of DMPO-$CH_3^{\bullet}CHOH$ adducts with $\alpha^N = 16.0$ G and $\alpha^H = 23.5$ G appeared (Fig. 8E). When mannitol (5 mM), a scavenger of hydroxyl radicals, was added into the solution prior to illumination, the signal did not appear. These suggested that DMPO-$^{\bullet}$OH was produced via the reaction between DMPO and $^{\bullet}$OH, instead of the decomposition of DMPO-$O_2^{\bullet-}$. The electron donors significantly enhanced the signal intensity of DMPO-$^{\bullet}$OH (Fig. 8D and Fig. 9 line 2). The concurrent

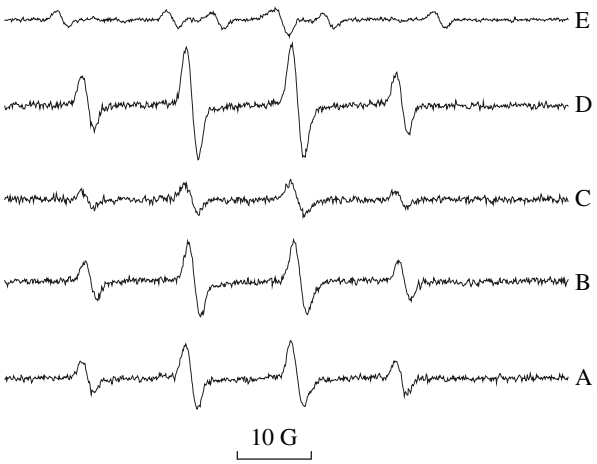

Fig. 8. (A) The EPR spectrum of DMPO-·OH adducts formed by irradiation of oxygen-saturated PBS solution (pH 7.4) containing SCHB (1 mM) and DMPO (50 mM). (B) The same as (A) but with 1.25 mM SCHB. (C) The same as (A) but in the presence of SOD (30 μg/mL). (D) The same as (A) but in the presence of NDAH (50 μM). (E) The same as (A) except that ethanol (0.1 M) was added prior to irradiation and then the sample was kept in the dark for 2 min.

enhancement effects of $O_2^{\cdot-}$ and ·OH suggested that $O_2^{\cdot-}$, in turn $SCHB^{\cdot-}$, should be the direct and indirect precursors of ·OH, respectively. No EPR signal was detected when catalase (50 μg/mL) was added, suggesting that the ·OH generation was H_2O_2 dependent.

SOD (30 μg/mL) inhibited the signal of DMPO-·OH (Fig. 8C and Fig. 9 line 3), suggesting involvement of $O_2^{\cdot-}$ in the formation of ·OH. When DTPA (up to 5 mM), a chelator of iron for preventing from further reaction with H_2O_2 [26], was added into the solution prior to illumination, the EPR signal of DMPO-·OH was inhibited but not disappeared completely (Fig. 10).

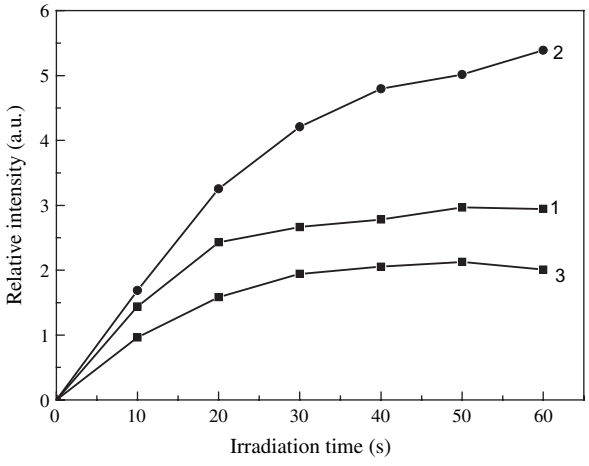

Fig. 9. Line 1: Dependence of the EPR signal intensity of DMPO-·OH on irradiation time in the oxygen-saturated PBS solution (pH 7.4) containing SCHB (1 mM) and DMPO (50 mM). Line 2: The same as line 1 except that NADH (50 μM) was added. Line 3: The same as line 1 except that SOD (30 μg/mL) was added.

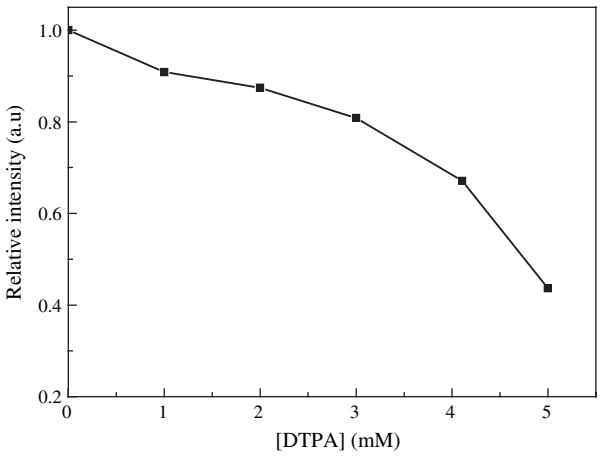

Fig. 10. Plot of the EPR signal intensities of DMPO-·OH against the concentrations of DTPA.

These observations suggested that hydroxyl radicals could be formed via not only the Fenton Haber–Weiss reaction or $O_2^{\cdot-}$-driven Fenton reaction but also the reaction (3).

$$SCHB^{\cdot-} + H_2O_2 \rightarrow SCHB + HO^{\cdot} + OH^- \quad (3)$$

Based on the above discussions, it can be suggested that ·OH is formed from H_2O_2, in turn formed via a rapid dismutation of $O_2^{\cdot-}$ to H_2O_2 and O_2. The inhibitory effect of catalase on the signal indicates that the photogeneration of ·OH is H_2O_2 dependent.

Briefly, it may be concluded that $SCHB^{\cdot-}$, $O_2^{\cdot-}$ and ·OH can be generated via the photosensitization of SCHB. Specially, the photogeneration of ·OH by SCHB was very efficient, which was not observed for the parent compound HBO_2H or HB.

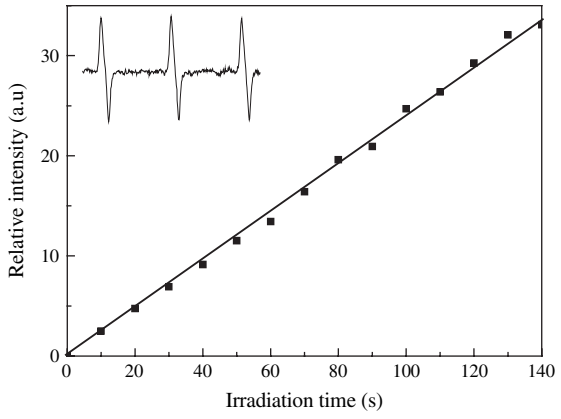

Fig. 11. The EPR signal intensity of TEMPO formed in an aerated PBS solution (pH 7.4) containing SCHB (1 mM) and TEMP (20 mM) under different irradiation time.

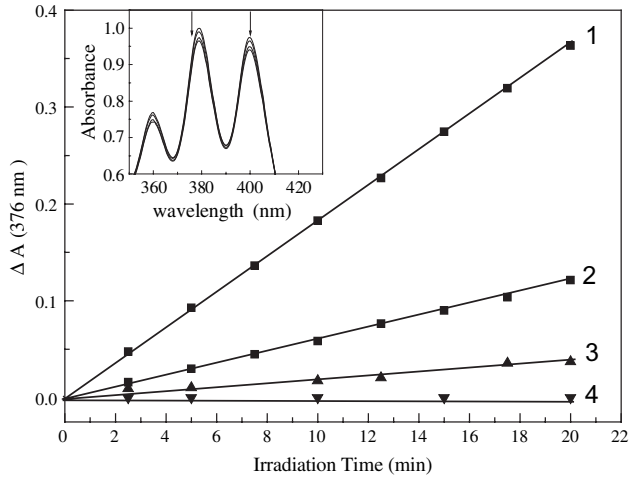

Fig. 12. Line 1: The differences in the absorbance of DPA (ΔA) at 376 nm under different irradiation time in an oxygen-saturated PBS solution (pH 7.4) containing RB and DPA. Line 2: The same as line 1 except that RB was replaced by SCHB. Line 3: Same as line 2 but with addition of DABCO or NaN_3 (5 mM). Line 4: The same as line 2 but in the absence of SCHB, oxygen or illumination. Inset: absorption spectra during the bleaching of DPA.

3.5. Formation of $^1O_2$ by SCHB

It was reported that TEMPO, an EPR-detectable nitroxide radical, was produced via the reaction of TEMP with singlet oxygen [27], which is usually used for monitoring the formation of singlet oxygen. When an oxygenated PBS solution containing SCHB (1 mM) and TEMP (20 mM) was illuminated at room temperature, a typical three-line EPR spectrum of TEMPO was observed (inset in Fig. 11). The signal intensity was dependent on the irradiation time (Fig. 11). Control experiment proved that SCHB, oxygen, light and TEMP were all necessary for the signal, supporting generation of $^1O_2$ via photosensitization of SCHB.

The DPA-bleaching method [28] was adopted to determine the quantum yield of $^1O_2$ produced by photosensitization of SCHB. Fig. 12 shows the photosensitized DPA-bleaching by SCHB (line 2) and Rose Bengal (RB) (line 1) in PBS solution (pH 7.4) under a series of irradiation time. During the measurements, the optical densities of the two dyes were adjusted to be the same at 496 nm. Control experiments proved that no DPA-bleaching would occur when the photosensitizer, oxygen or irradiation was absent (Fig. 12, line 4). The addition of DABCO or NaN_3 (10 mM), the $^1O_2$ quenchers, inhibited DPA-bleaching greatly (Fig. 12, line 3), further supporting the formation of singlet oxygen through energy transfer from triplet SCHB to molecular oxygen. The quantum yield of $^1O_2$ generated by the photosensitization of SCHB was estimated to be about 0.26 in PBS solution (pH 7.4) with RB (0.78) as reference in the aqueous solution [29,30].

4. Conclusion

In the current work, SCHB, a derivative of HB, was designed and prepared. The new derivative is soluble in aqueous PBS solution but also possesses a superior distribution in organic phase, which agrees very well with the theoretical prediction of the molecular polarity. Further, it was confirmed that $SCHB^{\bullet -}$, $O_2^{\bullet -}$, $^{\bullet}OH$ and $^1O_2$ could be generated through the photosensitization of SCHB. In aqueous solution, only $^{\bullet}OH$ was detected, which was not observed for the parent compound HBO_2H or HB in the similar conditions. Under the experimental conditions, $SCHB^{\bullet -}$, generated via the electron transfer between the triplet and the ground state of the photosensitizer molecules, was proved to be the main origin of $O_2^{\bullet -}$ which in turn was the precursor of $^{\bullet}OH$. It was observed that the photogenerated $SCHB^{\bullet -}$ would decay in second-order kinetics. The quantum yield for photogeneration of $^1O_2$, generated through energy transfer from the triplet SCHB to ground state oxygen molecules, was estimated to be about 0.26 in PBS solution (pH 7.4). It can be concluded that the photodynamic activity of SCHB involves in both Type I and Type II mechanisms. Owing to its good amphiphilicity (PC = 4.25) and photosensitive activity, the novel photosensitizer may be clinically usable for photodynamic therapy of some kinds of vascular–capillary diseases.

Acknowledgement

The Project supported by NSFC No 20273079.

References

[1] Diwu ZJ. Photochem Photobiol 1995;61(6):529.
[2] Miller GG, Brown K, Ballangrud AM, Barajas O, Xiao Z, Tulip J, et al. Photochem Photobiol 1997;65:714.
[3] Hudson JB, Zhou J, Harris L, Yip L, Towers GHN. Photochem Photobiol 1994;60:253.
[4] Hu YZ, An JY, Jiang LJ. J Photochem Photobiol B 1993;17:195.
[5] He YY, Liu HY, An JY, Han R, Jiang LJ. Dyes Pigments 2000; 44:63.
[6] Xie J, Ma JH, Zhao JQ. Sci China 2002;45:251.
[7] He YY, An JY, Zou W, Jiang LJ. J Photochem Photobiol B 1998; 44:45.
[8] Zhao KH, Jiang LJ. Chin J Org Chem 1992;10:339.
[9] He YY, An JY, Jiang LJ. J Photochem Photobiol A 1998;115:213.
[10] Hadjur C, Wagnieres G, Monnier P, van de Bergn H. Photochem Photobiol 1997;65:818.
[11] Hadjur C, Wagnieres G, Ihringer F, Monnier P, van de Bergn H. J Photochem Photobiol B 1997;38:196.
[12] Hu YZ, An JY, Jiang LJ, Chen DW. J Photochem Photobiol A 1995;89:45.
[13] Reszka K, Lown JW. Photochem Photobiol 1989;50:297.
[14] Harbour JR, Hair ML. J Phys Chem 1978;82:1397.

[15] Lissi EA, Encinas MV, Lemp E, Rubio MA. Chem Rev 1993; 93:699.
[16] He YY, An JY, Jiang LJ. Free Radic Biol Med 1999;26: 1146.
[17] Sanders SP, Harrison SJ, Kuppusamy P, Sylvester JT, Zweier JL. Free Radic Biol Med 1994;16:753.
[18] Fridovich I. In: Greenwald RA, editor. CRC handbook of methods for oxygen radical research. Boca Raton, FL: CRC Press; 1985. p. 121.
[19] Beyer WF, Fridovich I. Arch Biochem Biophys 1962;58:593.
[20] Hadjur C, Jardon P. J Photochem Photobiol B 1995;29:147.
[21] Hadjur C, Jeunet A, Jardon P. J Photochem Photobiol B 1994; 26:67.
[22] Finkelstein E, Rosen GM, Rauckman EJ. Arch Biochem Biophys 1980;200:1.
[23] Finkelstein E, Rosen GM, Rauckman EJ. J Am Chem Soc 1980; 102:4994.
[24] Lang K, Wangerova M, Stopka P, Dameran W. J Photochem Photobiol A 1992;67:187.
[25] Feix JB, Kalyanaraman B. Arch Biochem Biophys 1991;291:43.
[26] Halliwell B, Gutteridge JMC. Arch Biochem Biophys 1986;246:501.
[27] Lion Y, Delmelle M, Van de Vorst A. Nature 1976;263:442.
[28] Diwu ZJ, Lown JW. J Photochem Photobiol A 1992;64:273.
[29] He YY, Jiang LJ. Biochim Biophys Acta 2000;1523:29.
[30] Senthil V, Jones LR, Senthil K, Grossweiner LI. Photochem Photobiol 1994;59:40.